FEATURE ARTICLE

Catalysis with Transition Metal Nanoparticles in Colloidal Solution: Nanoparticle Shape Dependence and Stability

Radha Narayanan and Mostafa A. El-Sayed*

Laser Dynamics Laboratory, School of Chemistry and Biochemistry, Georgia Institute of Technology, Atlanta, Georgia 30332-0400

Received: March 2, 2005; In Final Form: April 14, 2005

While the nanocatalysis field has undergone an explosive growth during the past decade, there have been very few studies in the area of shape-dependent catalysis and the effect of the catalytic process on the shape and size of transition metal nanoparticles as well as their recycling potential. Metal nanoparticles of different shapes have different crystallographic facets and have different fraction of surface atoms on their corners and edges, which makes it interesting to study the effect of metal nanoparticle shape on the catalytic activity of various organic and inorganic reactions. Transition metal nanoparticles are attractive to use as catalysts due to their high surface-to-volume ratio compared to bulk catalytic materials, but their surface atoms could be so active that changes in the size and shape of the nanoparticles could occur during the course of their catalytic function, which could also affect their recycling potential. In this Feature Article, we review our work on the effect of the shape of the colloidal nanocatalyst on the catalytic activity as well as the effect of the catalytic process on the shape and size of the colloidal transition metal nanocatalysts and their recycling potential. These studies provide important clues on the mechanism of the reactions we studied and also can be very useful in the process of designing better catalysts in the future.

1. Introduction

Nanocatalysis is a rapidly growing field which involves the use of nanoparticles as catalysts for a variety of organic and inorganic reactions. Up until the end of 2004, there have been more than 2800 papers published in this field, and it has grown at an exponential rate during the past decade. Chemical reduction methods such as alcohol reduction,[1−7] hydrogen reduction,[8−13] sodium borohydride reduction,[14−18] etc. have been the most common ways of synthesizing colloidal metal nanoparticles. Other reduction methods such as electrochemical,[19−20] photochemical,[21−23] and sonochemical[24−26] reduction methods have also been used to a smaller extent. Many different stabilizers have been used as capping agents for the synthesis of colloidal metal nanocatalysts such as polymers,[1−13,27−28] dendrimers,[4,15,18,29−30] block copolymer micelles,[4,31−33] surfactants,[16,34−36] etc. Supported metal nanocatalysts have been prepared by the adsorption of the colloidal metal nanocatalysts onto the support,[37−46] grafting of the nanoparticles onto the support,[47−48] etc. Supported metal nanocatalysts can also be lithographically fabricated using electron beam lithography.[49−52] There have been numerous types of reactions that have been catalyzed using colloidal and supported metal nanocatalysts such as oxidations,[53−55] cross-coupling reactions,[2−4,6,13,18,56−60] electron-transfer reactions,[7,10−12,61−63] hydrogenations,[42−43,64−69] fuel cell reactions,[70−72] and many others. Numerous review articles have been published on the use of colloidal[73−80] and supported[81−93] transition metal nanoparticles as catalysts for a variety of organic and inorganic reactions.

It can be seen that transition metal nanoparticles are very attractive to use as catalysts due to their high surface-to-volume ratio and their high surface energy, which makes their surface atoms very active. However, having very active surface atoms could also result in the nanoparticles being unstable during the course of its catalytic function. This raises questions on whether the surface atoms are so active that they result in changes in the size and shape of the transition metal nanoparticles during their catalytic function. As a result, this also raises important questions on the recycling potential of the transition metal nanoparticles.

It is worth noting that there have been only a few studies reported in the literature on the characterization of the nanoparticles during and after catalysis and recycling. In these studies, the size distributions of the colloidal nanoparticles have been determined after the hydrogenation,[94−95] carbonylation,[96] and oxidation[97] reactions. In the hydrogenation of arenes with colloidal rhodium nanoparticles,[94] it was observed that no change in the size distribution or average size of the nanoparticles occurred after the reaction. However, HRTEM studies were not conducted to determine if changes in the morphology of the nanoparticles occurred. In the case of the enantioselective hydrogenation of ethyl pyruvate[95] where platinum nanoparticles were used as catalysts, it was observed that the nanoparticles were more monodisperse after the reaction. When palladium nanoparticles were used in low concentrations, it was also observed that the nanoparticles were more monodisperse after

* To whom correspondence should be addressed. Email: mostafa.el-sayed@chemistry.gatech.edu.

10.1021/jp051066p CCC: $30.25
Published on Web 06/04/2005

Radha Narayanan was born in Savannah, Georgia. She got her B.S. in Chemistry from Armstrong Atlantic State University and graduated *summa cum laude*. She has received numerous scholarships and fellowships during undergraduate and graduate studies such as HOPE scholarship, Governor's scholarship, Hodge scholarship, GAANN fellowship, Georgia Tech Presidential fellowship, etc. She graduated with a Ph.D. in chemistry in May 2005 under the direction of Professor Mostafa A. El-Sayed at Georgia Institute of Technology. Her Ph.D. research involved investigating the stability and recycling potential of different shaped colloidal transition metal nanoparticles during its catalytic function. She has compared the stability and catalytic activity of tetrahedral, cubic, and spherical platinum nanoparticles during the catalytic process. Her other research interests include the rational design of nanoparticles for various applications such as sensing, molecular transport, etc.

Professor Mostafa A. El-Sayed was born in Zifta, Egypt. He obtained his B.S. degree in Chemistry from Ain Shams University at Cairo, Egypt. He got his Ph.D. degree in Chemistry from Florida State University. During his Ph.D. studies, he worked with Professor Michael Kasha, Professor Ray Sheline, and Professor R. Wolfgang. He was a research associate at Harvard, Yale, and California Institute of Technology. In 1961, he was appointed to the faculty of University of California, Los Angeles. In 1994, he became the Julius Brown Chair in the School of Chemistry and Biochemistry at Georgia Institute of Technology. He is also the Regents' Professor and Director of the Laser Dynamics Laboratory at Georgia Tech. He has served as the Editor-in-Chief of Journal of Physical Chemistry from 1980−2004. He has received numerous fellowships such as Alfred P. Sloan Fellow, John Simon Guggenheim Fellow, Sherman Fairchild distinguished scholar, and Senior Alexander von Humboldt fellow. He was elected to the National Academy of Sciences and the Third World Academy of Science. He became an elected fellow of the American Academy of Arts and Sciences, the American Physical Society, and the American Association for the Advancement of Science. He has also received numerous national awards such as the Fresnius Award, McCoy Award, Harris Award, and the Irving Langmuir ACS National Award as well as the regional ACS awards in California, Southern California, Florida, Eastern Tennessee, and Northeastern sections. He has received the King Faisel International Award in Science and also received an honorary doctorate degree from Hebrew University. His research interests include understanding the optical properties and ultrafast dynamics of metal and semiconductor nanoparticles and the catalytic properties of transition metal nanoparticles of different shapes. His other research interests include the study of the primary processes involved in the photoisomerization and the proton pump in bacteriorhodopsin photosynthesis.

the reaction. However, when higher concentrations of the nanoparticles were used, it was observed that significant aggregation of the nanoparticles occurred after the catalytic process. In the case of the carbonylation of methanol catalyzed by rhodium nanoparticles,[96] the nanoparticles increased in size during the course of the reaction. The authors believed that catalysis did not take place on the surface of the nanoparticles. In the oxidation of L-sorbose,[97] it was observed that the platinum nanoparticles were larger in size after the reaction. The formation of enlarged platinum nanoparticles was attributed to the slow and continued reduction of the nanoparticles by the L-sorbose and also due to facilitated diffusion because of the swollen state of the HPS capping agent during the course of the reaction. The authors did not conduct a detailed examination on what causes these changes, and there is a possibility that Ostwald ripening is occurring.

For reactions catalyzed by metal nanoparticles in colloidal solution, there has not been any detailed examination reported in the literature on what causes the changes in the size distribution, the role of the individual chemicals present in the reaction mixture, and whether the changes in the nanoparticle shape and size affect the catalytic activity upon recycling. In addition, it is worth noting that there have not been any studies in the literature on what happens to the shape of *colloidal* metal nanoparticles after its catalytic function. This is also another important aspect to study. These kinds of studies can provide important clues on the mechanism of the catalytic reaction involved as well as provide directions for the design of better catalysts.

In the literature, there have not been many studies on recycling the nanoparticles for more catalytic cycles. In a review of transition metal colloids as reusable catalysts,[98] it was pointed out that the major interest of reusability of the nanoparticle catalysts has not been systematically studied or published in the metal colloid literature. Some studies in the literature that have examined the catalytic activity of the nanoparticles upon recycling, but which have not examined the stability of the nanoparticles, include reactions such as hydrogenation of alkenes,[99] Heck reaction between aryl halides and *n*-butyl-acrylate,[100] hydrogenation of olefins,[101] and hydrogenation of unsaturated fatty acid esters.[102] It is important to study the stability of these metal nanoparticles, and also their recycling potential, since it can also be affected by changes in the shape and size of the nanoparticles during the course of the reaction.

In this Feature article, we summarize the work we have conducted on examining the size and shape of colloidal platinum and palladium nanoparticles during the course of two different reactions. One reaction is the electron-transfer reaction between hexacyanoferrate (III) ions and thiosulfate ions to form hexacyanoferrate (II) ions and tetrathionate ions, which is carried out at room and different temperatures. The other reaction is the Suzuki cross-coupling reaction between phenylboronic acid and iodobenzene to form biphenyl, which takes place at 100 °C for 12 h. We start with our shape-dependent catalysis work

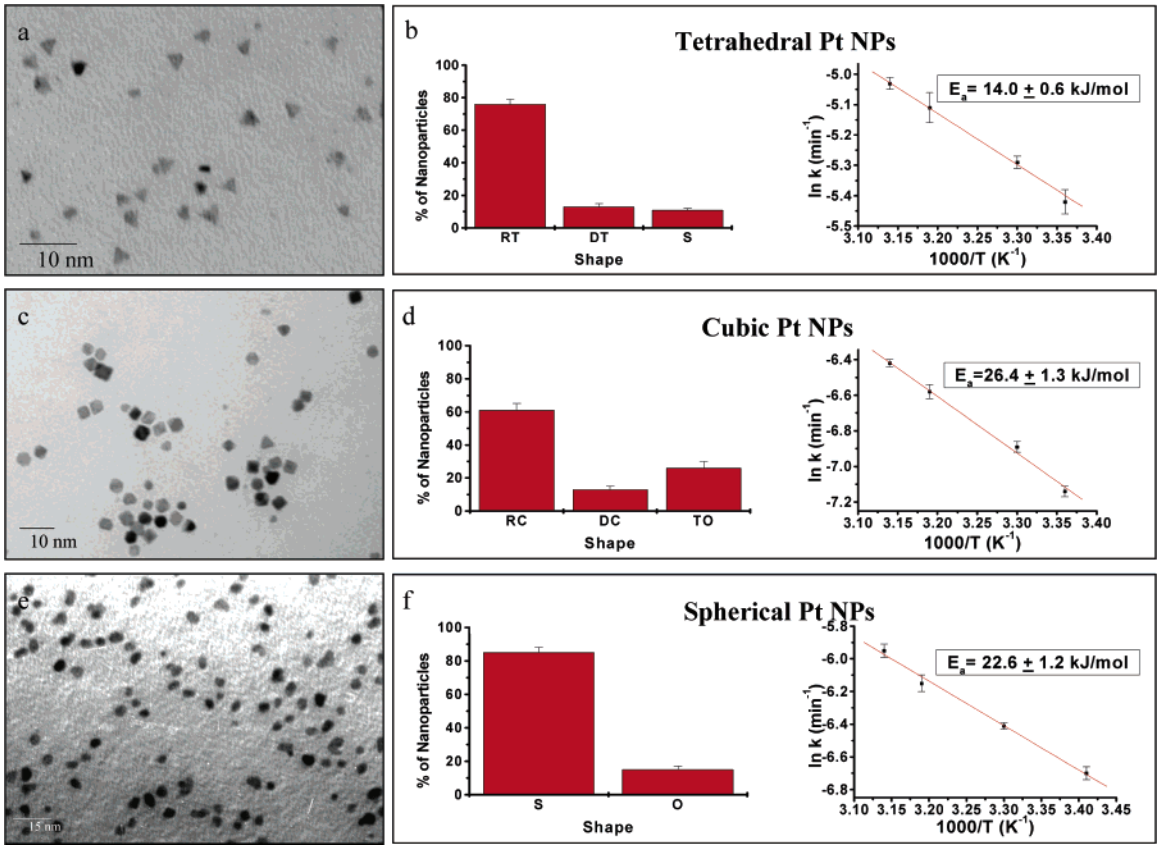

Figure 1. Shape-dependent catalytic activity. TEM images, shape distributions, and Arrhenius plots obtained with dominantly tetrahedral (a−b), cubic (c−d), and spherical (e−f) platinum nanoparticles.[11] It is observed that the tetrahedral platinum nanoparticles have the lowest activation energy, the cubic platinum nanoparticles have the highest activation energy, and the spherical platinum nanoparticles have an intermediate activation energy.

and then examine the effect of catalysis on the shape and size of the platinum nanoparticles during and after its catalytic function. We determined the activation energy in order to test the change in the nanocatalyst activity. We also discuss our work on examining the effect of catalysis on the size of spherical palladium and platinum nanoparticles. We have also examined the recycling potential of the tetrahedral platinum nanoparticles as well as the spherical platinum and palladium nanoparticles.

2. Shape-Dependent Nanocatalysis

The first report on the synthesis of platinum nanoparticles of different shapes (tetrahedral, cubic, and truncated octahedral)[8] appeared in 1996. Recently, there has been a lot of interest in the synthesis of platinum nanoparticles of different shapes such as tetrahedral,[8−13] cubic,[8,10−12,103] nanowire,[104] tetrapods,[105] etc. A modified version of the hydrogen reduction method using PVP (mw = 360 000) and the potassium hexachloroplatinate precursor salt has also been developed to prepare tetrahedral platinum nanoparticles.[9] Cubic platinum nanoparticles capped with oxalate have also been prepared using the hydrogen reduction method.[103] Modifications of the two previously discussed hydrogen reduction methods[8,9] have been used to prepare PVP capped tetrahedral platinum nanoparticles.[10−13] In addition, modification of the hydrogen reduction method[8] has been used to produce polyacrylate capped cubic platinum nanoparticles.[10−12] Platinum nanowires, tetrapods, and "sea urchins" have been synthesized using different modifications of the ethylene glycol reduction method and PVP as the capping agent.[104−105]

There have been very few studies in the literature on the use of nanoparticles of a specific shape to catalyze reactions. Truncated octahedral platinum nanoparticles have been used to catalyze the electron-transfer reaction.[61] The decomposition of oxalate has been catalyzed using cubic platinum nanoparticles.[103] There have not been any studies comparing the catalytic activity obtained using nanocatalysts of different shapes. Tetrahedral platinum nanoparticles are composed of (111) facets and have sharp corners and edges. Cubic platinum nanoparticles are composed of (100) facets and have corners and edges that are not as sharp as the tetrahedral ones. The spherical platinum nanoparticles are really "near spherical" in shape and are composed of numerous (111) and (100) facets with corners and edges located at the interfaces of these facets. As a result, it is worth comparing the catalytic efficiency of these different shaped platinum nanoparticles.

The tetrahedral platinum nanoparticles are synthesized by making modifications to the hydrogen reduction method[8,9] and are capped using the polyvinylpyrollidone (PVP) polymer.[10−12] The cubic platinum nanoparticles are also synthesized by making modifications to the hydrogen reduction method[8] and are capped using the polyacrylate capping agent.[10−12] The spherical platinum nanoparticles are synthesized using the ethanol reduction method[7] and are capped using PVP. Figure 1 shows TEM images and shape distributions of the tetrahedral, cubic, and spherical platinum nanoparticles used in the studies.[11] The dominantly tetrahedral nanoparticles have an average size of 4.8 ± 0.1 nm, the dominantly cubic nanoparticles have an average size of 7.1 ± 0.2 nm, and the dominantly spherical nanoparticles have an average size of 4.9 ± 0.1 nm.

In the literature, the electron-transfer reaction between hexacyanoferrate (III) ions and thiosulfate ions has been catalyzed using citrate capped spherical gold nanoparticles,[106−107] spherical

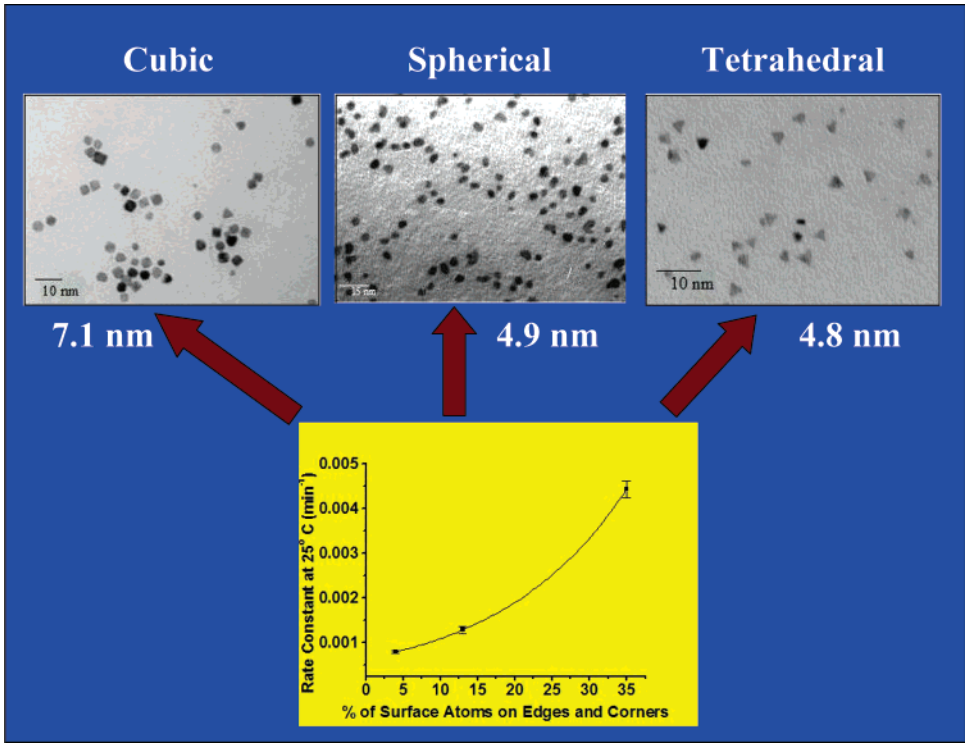

Figure 2. Correlation of catalytic activity with fraction of surface atoms on corners and edges. Plot of rate constant obtained at room temperature (25 °C) vs % surface atoms located on the corners and edges of the tetrahedral, cubic, and "near spherical" platinum nanoparticles.[11] It is observed that as the fraction of surface atoms located on the corners and edges increases, the rate constant also increases. The tetrahedral platinum nanoparticles have the highest fraction of surface atoms on the corners and edges and are also the most catalytically active.

platinum nanoparticles prepared in water-in-oil microemulsions,[108] and polyacrylate capped truncated octahedral platinum nanoparticles.[61] We used PVP capped tetrahedral, polyacrylate capped cubic, and PVP capped spherical platinum nanoparticles to catalyze the electron-transfer reaction.[10−12] This reaction takes place under moderate conditions (room temperature and pH = 7). The kinetics of this reaction is monitored by using absorption spectroscopy to follow the disappearance of the absorption of the hexacyanoferrate(III) ions at 420 nm with time. From this, the rate constant of the reaction is determined at different temperatures, from which the activation energy is determined. The change in reactivity for the three types of nanoparticles was monitored by following the change in the activation energy. The activation energy was obtained for the electron-transfer reaction from the Arrhenius plot determined from the kinetics of the reaction during the first forty minutes at four different temperatures.[11] Using a longer time frame was found to give differences in the reactivity with the shape as a result of dissolution of the corner and edge atoms of the different nanoparticles,[12] and this is discussed later on in this article. The shape distribution of the nanoparticles was obtained after the first 40 min of the electron transfer reaction, and it was determined that there are negligible differences in the shape distribution during this relatively short time frame. As a result, determining the activation energy based on the kinetics during the first forty minutes is a good time frame to determine the effect of the nanoparticle shape on the catalytic activity. As can be seen in Figure 1, the activation energy of the reaction is lowest when tetrahedral platinum nanoparticles are used as the catalyst, while it is the highest when cubic platinum nanoparticles are used as the catalyst.[11] An intermediate activation energy is obtained when spherical platinum nanoparticles are used as catalysts.

TABLE 1: Comparison of the Fraction of Active Surface Sites (fraction of surface atoms located on the defective corners and edges) and the Activation Energy for the Three Different Types of Nanoparticles[11]

nanoparticle shape	nanoparticle size (nm)	fraction of active surface sites (%)	activation energy (kJ/mol)
dominantly tetrahedral (76%)	4.8 ± 0.1	35	14.0 ± 0.6
dominantly cubic (61%)	7.1 ± 0.2	4	26.4 ± 1.3
dominantly "near spherical" (85%)	4.9 ± 0.1	13	22.6 ± 1.2

3. Dependence of Catalytic Activity on Fraction of Surface Atoms on Corners and Edges

Since the average size of each of the three different shaped platinum nanoparticles is not the same, the fraction of surface atoms on the corners and edges of each type of nanoparticle is also determined. This gives a much more accurate indication of the catalytic activity for the three types of nanoparticles since the formulas take into account both the size and the shape of the nanoparticles. This is shown to be easily done using formulas based on the tetrahedron model, cubic model, and cubo-octahedron model.[109] The cubo-octohedron model is used for the spherical nanoparticles since they are really "near spherical" in shape and composed of numerous corners and edges at the interfaces of the (100) and (111) facets.

As can be seen in Table 1, the PVP-capped tetrahedral platinum nanoparticles have the greatest fraction of surface atoms on the corners and edges and also have the lowest activation energy.[11] This suggests that the tetrahedral platinum nanoparticles are the most catalytically active. The polyacrylate capped cubic platinum nanoparticles have the lowest fraction of surface atoms located on the corners and edges and also have

the highest activation energy, suggesting that they are the least catalytically active. The PVP capped "near spherical" platinum nanoparticles have an intermediate fraction of active surface sites and an intermediate activation energy. In addition, Figure 2 shows a plot of the rate constant obtained at room temperature (25 °C) for the different shaped nanoparticles vs the % surface atoms located on the corners and edges.[11] It correlates the three different shaped nanoparticles with the fraction of surface atoms located on the corners and edges. It can be seen that the tetrahedral Pt nanoparticles have the highest fraction of surface atoms located on the corners and edges and also have the highest rate constant, suggesting that the tetrahedral Pt nanoparticles are the most catalytically active.

4. Effect of Catalysis on the Shape and Size of Different Shaped Platinum Nanoparticles

In this section, we discuss the effect of catalyzing the full course of the electron-transfer reaction (2 days) on the shape of the PVP-capped tetrahedral, polyacrylate-capped cubic, and PVP-capped spherical platinum nanoparticles and their catalytic activity.[10,12] The effect of individual reactants on the nanoparticle shape is discussed. We also show the effect of catalyzing the Suzuki cross-coupling reaction on the shape and size of tetrahedral platinum nanoparticles.[13] The effect of shape and size changes on the recycling potential of the platinum nanoparticles for the Suzuki reaction is discussed.

4.1. Tetrahedral, Cubic, and Spherical Platinum Nanoparticles Catalyzing the Electron-Transfer Reaction. We followed the shape distribution of the PVP-capped tetrahedral, polyacrylate-capped cubic, and PVP-capped spherical platinum nanoparticles at different time periods during the full course of the electron-transfer reaction (2 days).[12] It is observed that dissolution of platinum atoms occurred on the corners and edges of the tetrahedral and cubic platinum nanoparticles. This results in the formation of distorted tetrahedral and distorted cubic platinum nanoparticles. As can be seen in Figure 3, the rate of shape changes is faster for the tetrahedral platinum nanoparticles than for the cubic platinum nanoparticles.[12] This is because the tetrahedral nanoparticles have sharper corners and edges and also have a greater fraction of surface atoms located on their corners and edges. The kinetics of the reaction was followed at different time periods during the full course of the reaction, and Arrhenius plots were obtained for each time period to determine the activation energy. It is observed that there is a corresponding change in the activation energy that occurs along with changes in the shape during the course of the reaction.[12] The tetrahedral and cubic platinum nanoparticles strive to behave like the spherical platinum nanoparticles since they have the lowest surface energy. Combining the results in Figure 2 and those in Figure 3, one reaches the important conclusion that for nanocatalysts of comparable sizes, *the "near spherical" nanoparticles are of modest catalytic activity and are the most stable*.

We also examined the shape distribution of the tetrahedral and cubic platinum nanoparticles after the first and second cycle of the electron-transfer reaction by using TEM.[10] The distorted tetrahedral nanoparticles are dominant after the first cycle of the electron transfer reaction, while the distorted cubic platinum nanoparticles are dominant only after the second cycle of the electron-transfer reaction. This also shows that the rate of shape changes is faster in the case of the tetrahedral platinum nanoparticles than the cubic platinum nanoparticles. As a result, the tetrahedral platinum nanoparticles are more sensitive and liable to shape changes than the cubic platinum nanoparticles.

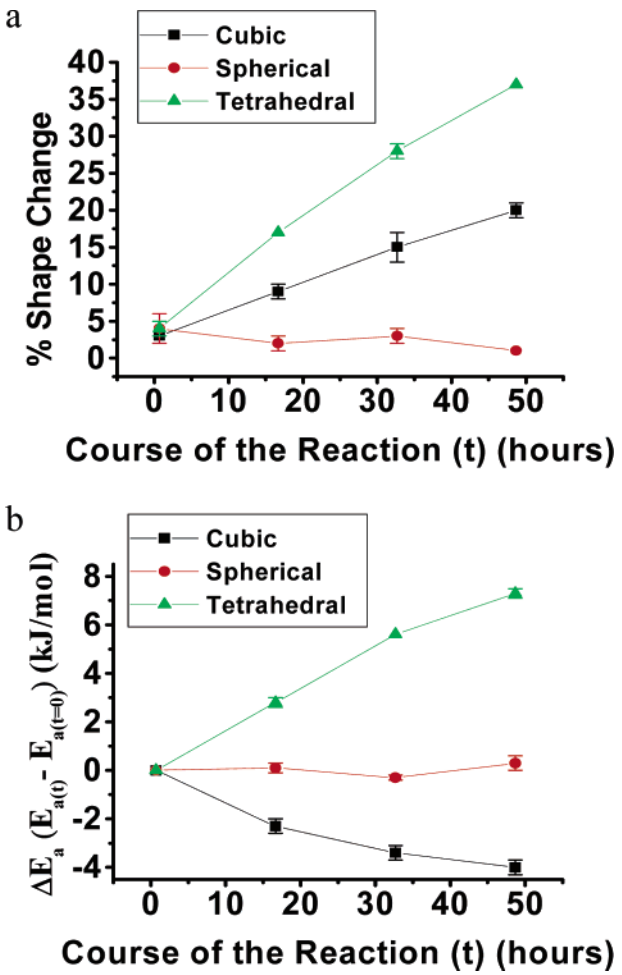

Figure 3. Rate of shape and activation energy changes during the course of the electron-transfer reaction. Percent change in the shape of the three types of platinum nanoparticles during the course of the electron-transfer reaction (a) and the change in the activation energy (b).[12] It is observed that the rate of shape change is faster for the tetrahedral Pt nanoparticles than the cubic Pt nanoparticles. There is a corresponding change in the activation energy that occurs for both the tetrahedral and the cubic platinum nanoparticles in which they strive to behave more like spherical nanoparticles. From this figure, one concludes that for comparable sized nanoparticles, the "near spherical" nanoparticles are of modest catalytic activity and are the most stable.

We also obtained HRTEM images[10] of the tetrahedral and cubic platinum nanoparticles before and after the electron-transfer reaction as shown in Figure 4. It can be seen that there is a greater amount of distortion that occurs in the tetrahedral platinum nanoparticle than in the cubic platinum nanoparticle after the electron-transfer reaction.

We also conducted a study on the effect of the individual reactants on the tetrahedral and cubic platinum nanoparticles.[10] When the nanoparticles are exposed to just the hexacyanoferrate(III) ions, it is observed that there is great distortion of the corner and edge atoms that occurs for both the tetrahedral and cubic nanoparticles, but there is more rapid dissolution of corner and edge atoms that occurs for the tetrahedral nanoparticles than for the cubic platinum nanoparticles. In the case of the cubic nanoparticles, even though the (100) facets are less sensitive to perturbations, dissolution of atoms on the reactive corners and edges is probably faster than on the faces. The hexacyanoferrate(III) ions probably attack the nanoparticle surface at the corners and edges, resulting in dissolution of those Pt atoms, which can then form a complex via the CN^- ligand. This is a reasonable explanation for the shape changes since

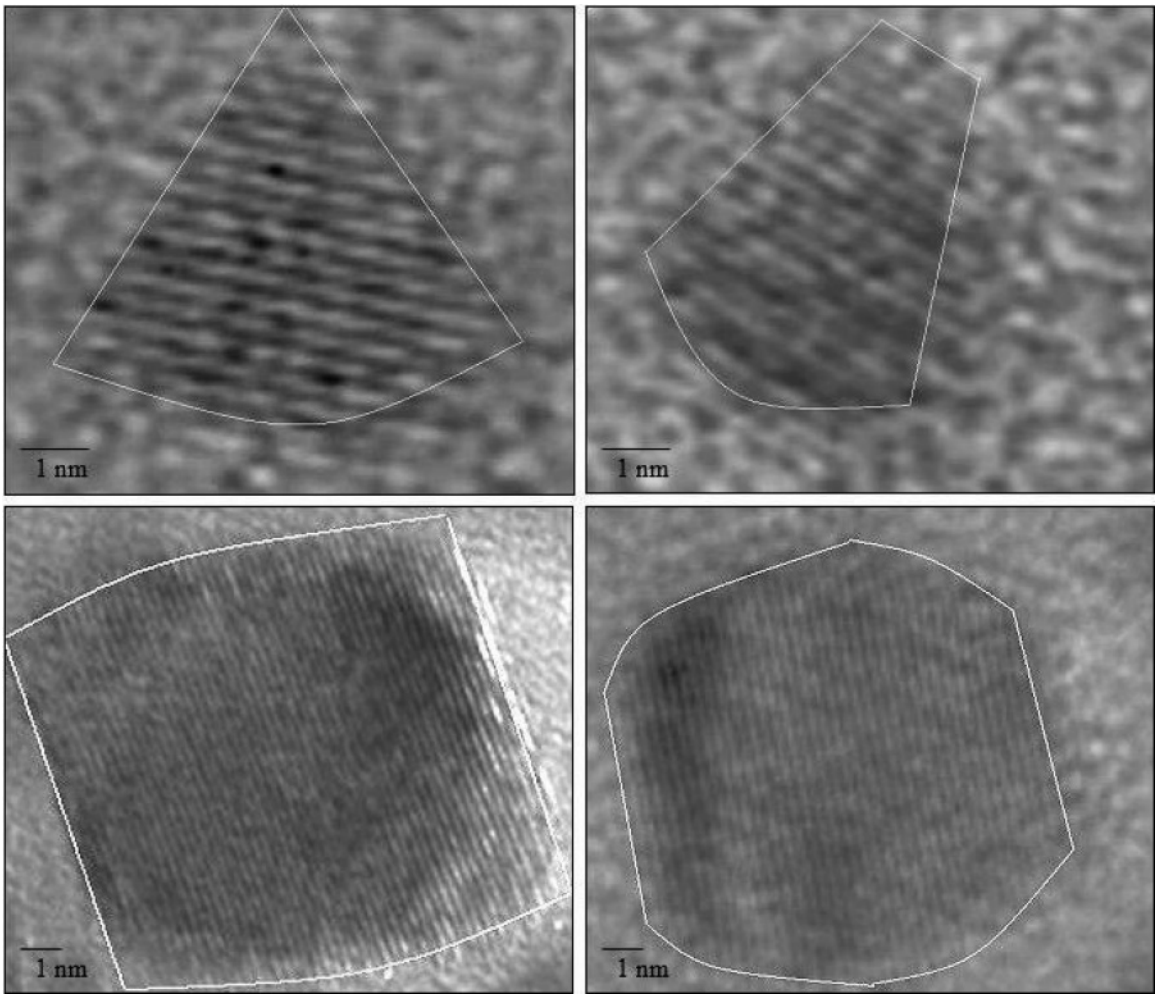

Figure 4. High-resolution TEM images showing shape changes. HRTEM images of a tetrahedral (a−b) and cubic (c−d) platinum nanoparticle before and after the electron-transfer reaction. The nanoparticles are outlined in order to see their shape more clearly.[10] The shape changes that occur after the electron-transfer reaction for the tetrahedral nanoparticle and the cubic nanoparticle can be seen in greater detail. The tetrahedral nanoparticle becomes smaller in size and strives toward the spherical shape. More corner and edge sites are formed in the case of the cubic nanoparticle.

the stability constant of the platinum complex is 10 orders of magnitude higher than that of the iron complex. In the case where the nanoparticles are exposed to thiosulfate ions, it is observed that both the tetrahedral and cubic platinum nanoparticles maintain their stability. These observations suggest that the mechanism of the electron-transfer reaction involves the thiosulfate ions binding to the nanoparticle surface and reacting with the hexacyanoferrate (III) ions in solution.[10] This agrees with the mechanism we proposed previously in our studies with the spherical Pt nanoparticles catalyzing the electron-transfer reaction,[7] which we discuss later on in the feature article. Overall, this suggests that the mechanism of the reaction is not dependent on the shape of the nanocatalyst.

4.2. Tetrahedral Platinum Nanoparticles Catalyzing the Suzuki Reaction. The Suzuki cross-coupling reaction is an effective synthetic route for the production of biaryls by the coupling of arylboronic acids with haloarenes. It was discovered by A. Suzuki in 1981 and is sometimes referred to as the Suzuki−Miyaura coupling reaction.[110] Suzuki reactions have been traditionally catalyzed using many different kinds of phosphine-based palladium catalysts and phosphine-free palladium complexes such as $Pd(PPh_3)_4$, $Pd(Oac)_2$, $[(n^3\text{-}C_3H_5)\text{-}PdCl]_2$, $Pd_2(dba)_3$ C_6H_6, etc.[111−115] The use of palladium nanoparticles as catalysts for Suzuki reactions has been a fairly recent phenomenon. Palladium nanoparticles stabilized with tetraalkylammonium salts,[116] PVP,[2−3,6] PANAM dendrimers,[4,18] PS-*b*-PANa block copolymer,[4] 1,5-Bis(4,4′-bis(perfluorooctyl)-phenyl)-1,4-pentadien-3-one,[117] Keggin-type polyoxometalate[118] and cyclodextrin[119] have all been used to catalyze various Suzuki reactions. It is worth noting that it has been shown very recently that platinum complexes such as $[PtCl_2\text{-}(NCPh)_2]$ and $K_2[PtCl_4]$ can also be used as catalysts for the Suzuki reaction.[120] There has been one study that has shown that spherical platinum nanoparticles do not catalyze the Suzuki reaction.[121] As a result, it would be interesting to see if the PVP-capped tetrahedral platinum nanoparticles with their high fraction of surface atoms on corners and edges can catalyze the Suzuki reaction. In addition, the effect of catalyzing a harsh reaction such as the Suzuki reaction on the tetrahedral shape can also be investigated.

We have used PVP-capped tetrahedral platinum nanoparticles to catalyze the Suzuki cross-coupling reaction between phenylboronic acid and iodobenzene to form biphenyl.[13] This reaction is a relatively harsh one since it takes place at 100 °C for 12 h. The reaction also takes place in the presence of sodium acetate, which is necessary to activate it. Reversed-phase HPLC was used to monitor the biphenyl product yield after the first and second cycle of the Suzuki reaction. As shown in Table 2, it was observed that while the tetrahedral platinum nanoparticles are able to catalyze the Suzuki reaction,[13] they are much less catalytically active than the spherical palladium nanoparticles

TABLE 2: Summary of the Concentration and % Yield of Biphenyl Obtained Using the Tetrahedral PVP−Pt Nanoparticles[13] and the Spherical PVP−Pd Nanoparticles[6]

condition	concentration (mM) and % yield of biphenyl using tetrahedral PVP−Pt nanoparticles[13]	concentration (mM) and % yield of biphenyl using spherical PVP−Pd nanoparticles[6]
first cycle of Suzuki reaction	1.07 ± 0.05 mM 14 ± 5%	3.00 ± 0.32 mM 39 ± 4%
second cycle of Suzuki reaction	0.36 ± 0.03 mM 5 ± 2%	1.11 ± 0.20 mM 15 ± 3%

we studied previously.[6] After the first cycle of the Suzuki reaction,[13] we observed that the dominantly tetrahedral platinum nanoparticles transform into similarly sized spherical platinum nanoparticles, as can be seen in Figure 5. After the second cycle of the Suzuki reaction, we also observed that the transformed spherical platinum nanoparticles become larger in size. This could be attributed to Ostwald ripening,[122−123] which is a mechanism of cluster growth in which atoms on the smaller nanoparticle surfaces dissolve and deposit on the more stable surfaces of the larger nanoparticles. In addition, the presence of unreduced and partly reduced Pt ions and Pt atoms present in solution can also contribute to the growth of the nanoparticles. When the nanoparticles are recycled, it is observed that the biphenyl product yield is very small as shown in Table 2, suggesting that the transformed spherical platinum nanoparticles do not catalyze the Suzuki reaction.[13] This is in agreement with the results reported in the literature[121] where it was shown that spherical platinum nanoparticles do not catalyze the Suzuki reaction.

We also conducted studies on the effect of individual reactants on the shape and size of these tetrahedral platinum nanoparticles.[13] When the tetrahedral platinum nanoparticles are refluxed in the solvent alone, the transformation to dominantly spherical platinum nanoparticles does take place, suggesting that the Ostwald ripening process occurs. It is observed that when the nanoparticles are refluxed in the presence of iodobenzene, the tetrahedral nanoparticles transform into similarly sized spherical platinum nanoparticles. This suggests that the iodobenzene does not interact with the nanoparticle surface. When the nanoparticles are refluxed in the presence of phenylboronic acid, it is observed that the tetrahedral nanoparticles remain the dominant shape and do not change in size. As a result, the presence of phenylboronic acid inhibits the shape transformation process. This could be due to it binding to the nanoparticle surface via the O^- in the OH group when it is in the deprotonated form due to the presence of the sodium acetate base. These observations suggest that the mechanism of the Suzuki reaction involves the phenylboronic acid binding to the platinum nanoparticle surface and reacting with iodobenzene

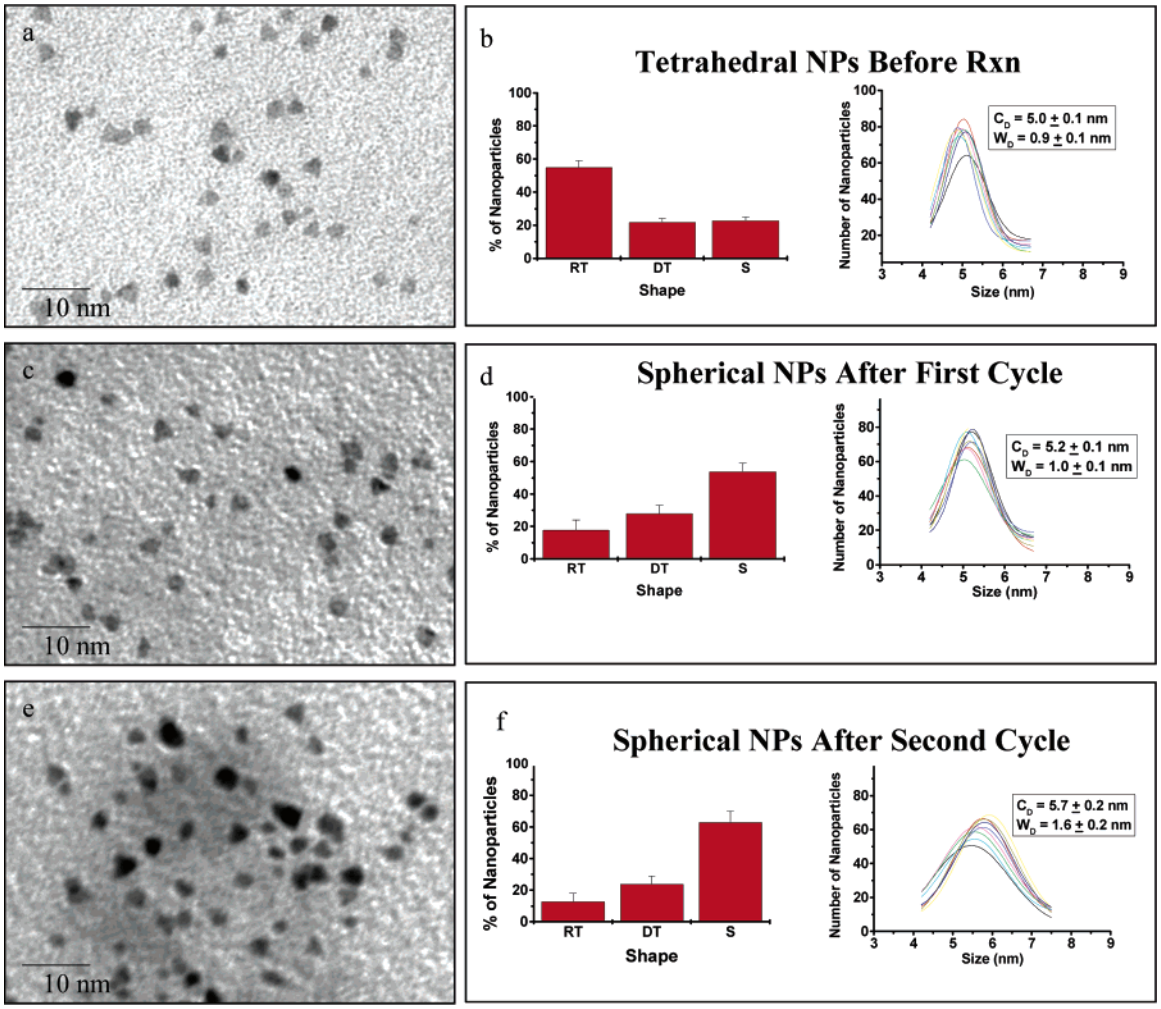

Figure 5. Shape transformation of the tetrahedral platinum nanoparticles during the Suzuki reaction. TEM images, shape distributions, and size distributions of the dominant nanoparticle shape before the Suzuki reaction (a−b), after the first cycle of the Suzuki reaction (c−d), and after the second cycle of the Suzuki reaction (e−f).[13] It can be seen that the dominantly tetrahedral platinum nanoparticles transform to spherical shaped platinum nanoparticles after the first cycle of the Suzuki reaction. After the second cycle, the transformed spherical platinum nanoparticles grow in size due to the Ostwald ripening process.

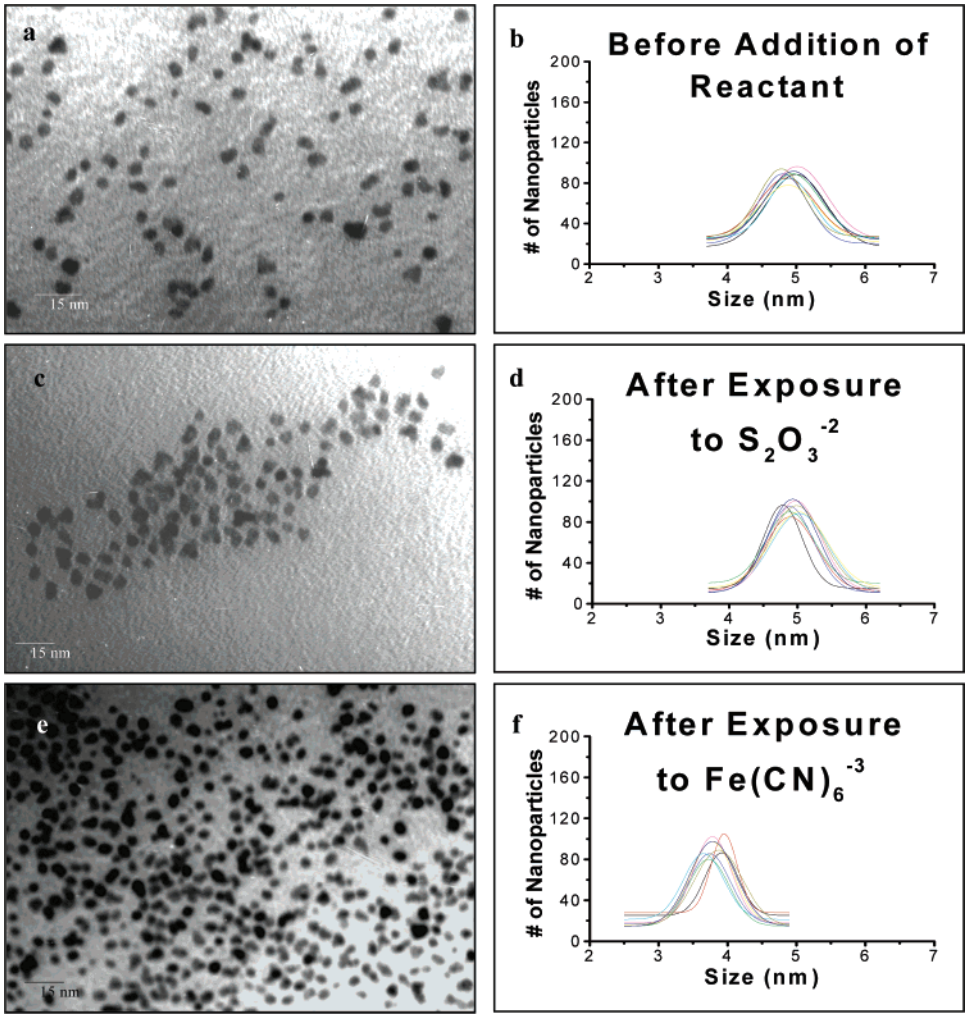

Figure 6. Effect of individual reactants on the size of spherical platinum nanoparticles. TEM images and Gaussian fits of the size distributions of the PVP-capped platinum nanoparticles before any perturbations (a−b), after exposure to just the thiosulfate ions (c−d), and after exposure to just the hexacyanoferrate(III) ions (e−f).[7] The presence of only the thiosulfate ions results in the nanoparticles maintaining their size while the presence of only the hexacyanoferrate(III) ions results in a reduction of the nanoparticle size.

in solution. This agrees with the Suzuki reaction mechanism we proposed previously based on our studies with the spherical palladium nanoparticles,[6] which we will discuss later in this article. This also suggests that the mechanism of the Suzuki reaction does not depend on the shape of the transition metal nanocatalyst.

5. Effect of Catalysis and Individual Reactants on the Size of Spherical Platinum and Palladium Nanoparticles

We have conducted detailed studies on the effect of catalysis and the individual reactants on the size of the spherical PVP−Pt nanoparticles catalyzing the electron-transfer reaction between hexacyanoferrate(III) ions and thiosulfate ions[7] and the spherical PVP−Pd nanoparticles catalyzing the Suzuki cross-coupling reaction between phenylboronic acid and iodobenzene.[6] The studies on the effect of exposing the nanoparticles to the individual reactants on the size of the platinum and palladium nanoparticles have provided important clues on the mechanisms of both reactions. The recycling potential of the palladium and platinum nanoparticles in both reactions were also investigated.

5.1. Spherical Platinum Nanoparticles Catalyzing the Electron-Transfer Reaction. We have used spherical platinum nanoparticles synthesized by the ethanol reduction method and capped with PVP as catalysts for the electron-transfer reaction between hexacyanoferrate(III) ions and thiosulfate ions.[7] These platinum nanoparticles have an average size of 4.9 ± 0.1 nm. After the first and second cycle of the electron transfer reaction, we observed that that there is a slight reduction in the size of the nanoparticles and the size distribution is slightly more monodisperse.

We also conducted studies on the effect of the individual reactants on the size of the spherical platinum nanoparticles.[7] When the PVP−Pt nanoparticles are exposed to just the hexacyanoferrate(III) ions,[7] it is observed that there is a great reduction in the size of the nanoparticles as can be seen in Figure 6. This could be explained by the hexacyanoferrate(III) ions attacking the platinum nanoparticle surface, resulting in dissolution of platinum atoms from the nanoparticle surface. The platinum atoms could then form a complex via the CN^- ligand present in hexacyanoferrate(III) ions. This is a logical possibility since the stability constant for the platinum complex is 10 orders of magnitude higher than that of the iron complex. We also calculated the amount of hexacyanoferrate(III) ions that could be lost due to the formation of the complex, which is 0.12% of the initial concentration and also too small to be detected by absorption spectroscopy. When the nanoparticles are exposed to just the thiosulfate ions,[7] it is observed that there is no change in their size, suggesting that the nanoparticles maintain their

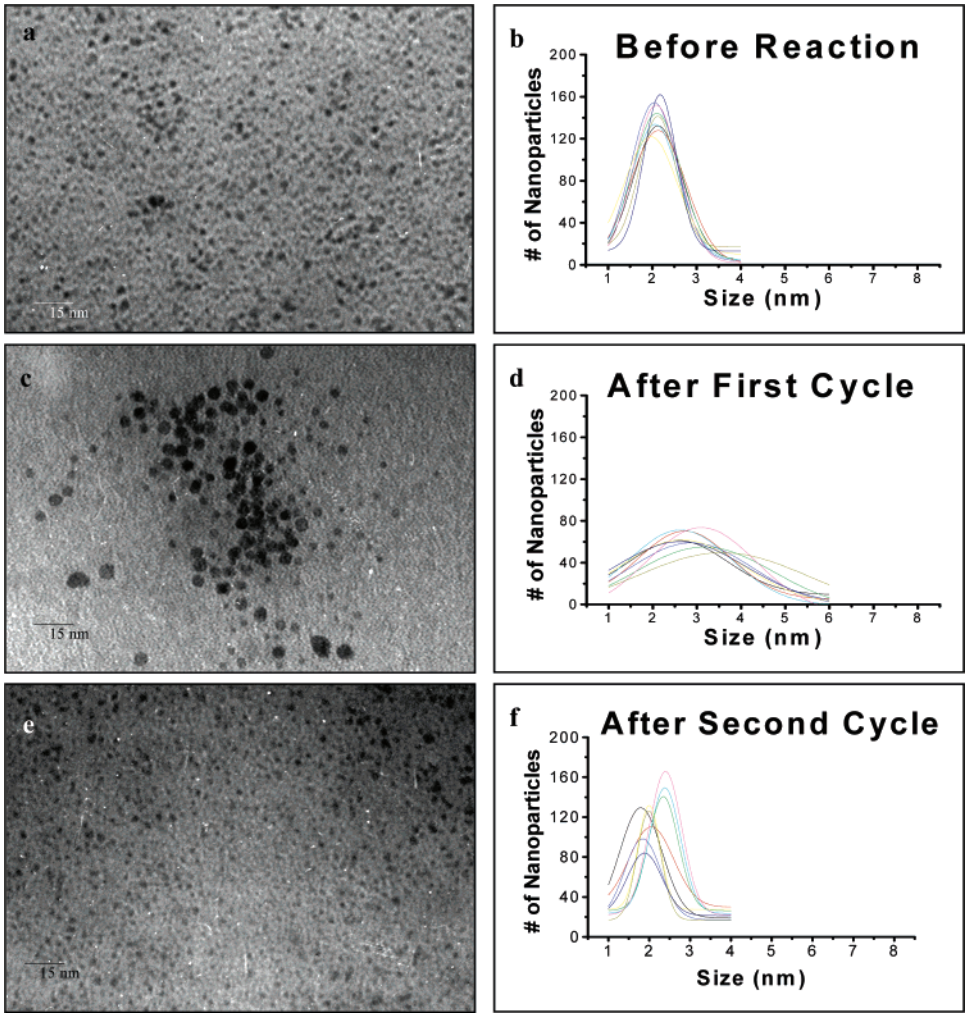

Figure 7. Effect of catalyzing the Suzuki reaction on the size of spherical PVP-capped palladium nanoparticles. TEM images and Gaussian fits of the size distributions of the spherical PVP−Pd nanoparticles before the reaction (a−b), after the first cycle (c−d), and after the second cycle (e−f).[6] It is observed that the palladium nanoparticles grow larger in size after the first cycle of the Suzuki reaction due to the Ostwald ripening process. The larger nanoparticles formed during the first cycle aggregate and precipitate out of solution, resulting in the smaller nanoparticles remaining in solution after the second cycle.

stability as shown in Figure 6. This is plausible since the thiosulfate ions could bind to the nanoparticle surface via the S^- group.

Based on these observations, the mechanism of the electron-transfer reaction involves the thiosulfate ions binding to the platinum nanoparticle surface and reacting with hexacyanoferrate(III) ions via collisional processes.[7] During the reaction, the thiosulfate ions bind to the nanoparticle surface and passivate it from attack from the hexacyanoferrate(III) ions. As a result, the hexacyanoferrate(III) ions react with the surface bound thiosulfate ions to form the products. This explains why there is only a small change in the size distribution of the nanoparticles after the first and second cycle of the electron-transfer reaction.

The kinetics of the electron-transfer reaction was followed by monitoring the disappearance of hexacyanoferrate(III) ions at 420 nm over time by absorption spectroscopy. The rate constants obtained during the first 40 min of the first cycle were compared to that obtained during the first 40 min of the second cycle in order to find out if recycling the spherical PVP−Pt nanoparticles has any effect on the catalytic activity. It was observed that the rate constants are similar for both cycles of the electron-transfer reaction. This suggests that the spherical PVP-capped platinum nanoparticles are recyclable for a mild reaction such as the electron-transfer reaction.

The activation energy of the reaction was also determined for four different concentrations of the spherical PVP-capped platinum nanoparticles by following the kinetics of the electron-transfer reaction during the first 40 min at four different temperatures (25, 30, 40, and 45 °C). An interesting trend was observed in which the activation energy decreases linearly with increasing PVP−Pt nanoparticle concentration.[7] This trend also occurs during the second cycle of the electron transfer reaction. This suggests that the nature of the catalytic particles changes with the concentration due to aggregation. The type of catalytic particles changes as new sites created at the intersection of the aggregated nanoparticles are formed. As a result, it is possible that atoms at these sites are more catalytically active, giving rise to a reduction in the activation energy that is observed in the more concentrated nanoparticle solutions.

5.2. Spherical Palladium Nanoparticles Catalyzing the Suzuki Cross-Coupling Reaction. We have used PVP-capped palladium nanoparticles to catalyze the Suzuki cross-coupling reaction between phenylboronic acid and iodobenzene to form biphenyl.[6] The spherical PVP−Pd nanoparticles have an average size of 2.1 ± 0.1 nm. After the first cycle of the Suzuki reaction,[6] it is observed that the palladium nanoparticles become larger in size and the width of the size distribution is very broad as can be seen in Figure 7. We attribute the growth of the

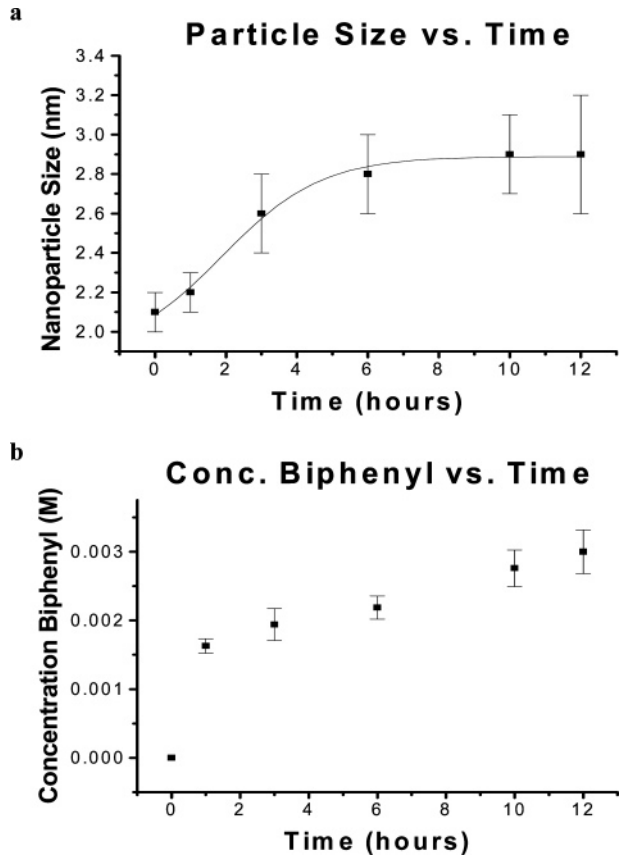

Figure 8. Growth of the palladium nanoparticles and concentration of biphenyl product over time. Average size of the PVP−Pd nanoparticles over the course of the first cycle of the Suzuki reaction (a) and concentration of biphenyl during the course of the first cycle of the Suzuki reaction (b).[6] Most of the growth of the nanoparticles occurs during the first 3 h and the growth levels off after this time period. There is a lot of biphenyl formed during the first hour, and the rate of formation of biphenyl is much lower during the rest of the time period.

nanoparticles to the Ostwald ripening process as well as the presence of unreduced and partly reduced palladium ions and palladium atoms. The Ostwald ripening process is a mechanism of cluster growth in which there is detachment of surface atoms from the smaller nanoparticles, followed by reattachment of these atoms to the more stable surfaces of the larger nanoparticles. In the literature,[124−128] it is shown that the mechanism of nanoparticle growth is the Ostwald ripening process when the reduction process takes place at high temperatures. In this case, a broad size distribution of the nanoparticles is observed. Because of this and the shape of the size distribution curve we observe for the palladium nanoparticles after the first cycle of the Suzuki reaction (Figure 7d), we conclude that the change in the particle size distribution is dominantly due to the Ostwald ripening process. After the second cycle of the Suzuki reaction, it is observed that the nanoparticles become much smaller in size and are monodisperse. This could be due to the larger nanoparticles formed in the first cycle aggregating and precipitating out of solution, resulting in the smaller nanoparticles remaining in solution. Pd black precipitate is observed after the second cycle of the reaction, and this supports our TEM observations.

The size distribution of the spherical PVP−Pd nanoparticles was also determined at different time periods during the first cycle of the Suzuki reaction.[6] As can be seen in Figure 8, it is observed that most of the growth of the nanoparticles due to the Ostwald ripening process takes place during the first 3 h, and then levels off toward the end of the first cycle due to the depletion of small nanoparticles as well as Pd atoms in solution.[6] The formation of biphenyl during this time period was also monitored as shown in Figure 8. It is observed that there is rapid formation of biphenyl during the first hour of the reaction and the formation of biphenyl is very slow afterwards. The slow formation of biphenyl after the first hour could be due to the nanoparticles becoming larger in size and also due to poisoning of the nanoparticles because of the biphenyl product itself.[6]

Studies on the effect of individual reactants[6] on the nanoparticle size were carried out and the results are shown in Figure 9. When the PVP−Pd nanoparticles are refluxed in the presence of just the 3:1 acetonitrile/water solvent, it is observed that the Ostwald ripening process takes place more effectively than during the reaction process. When the nanoparticles are refluxed in the presence of the phenylboronic acid + sodium acetate, it is observed that the Ostwald ripening process is inhibited since the nanoparticles do not grow in size. This could be due to the phenylboronic acid being in the deprotonated form in the presence of sodium acetate and binding to the nanoparticle surface and acting as a capping agent. It is worth noting that the Ostwald ripening process is inhibited when the nanoparticles are refluxed in the presence of the phenylboronic acid, but not when the nanoparticles are refluxed in the solvent alone. The observation suggests that the adsorbed capping material is in dynamic equilibrium with its species in solution. If one of the reactants can bind the surface, it could shift the equilibrium of the capping molecules toward the free species. In other words, in the reactions that are catalyzed with the nanoparticles in colloidal solution, one requirement will be that one (or both) reactant binds to the surface more strongly than the capping material used. In the Suzuki reaction, it is phenylboronic acid that binds to the nanoparticle surface, and in the electron-transfer reaction, it is the thiosulfate ion.

When the nanoparticles are refluxed in the presence of iodobenzene + sodium acetate, the Ostwald ripening process is observed to occur, suggesting that it probably does not interact with the nanoparticle surface. These observations suggest that the mechanism of the Suzuki reaction involves the phenylboronic acid binding to the nanoparticle surface and reacting with iodobenzene via collisional processes.[6]

The recycling potential of the spherical PVP-capped palladium nanoparticles was also investigated. As can be seen in Table 2, the biphenyl yield during the second cycle of the reaction is much lower than during the first cycle.[6] This could be due to the lower concentration of nanoparticles present in solution during the second cycle because of aggregation and precipitation of the larger nanoparticles formed in the first cycle and possible surface poisoning by the products. The great reduction in the catalytic activity of the palladium nanoparticles during the second cycle suggests that the PVP−Pd nanoparticles are not very efficient catalysts in terms of recycling potential.

6. Effect of Stabilizer on the Palladium Nanoparticle Size after the Catalytic Process

A comparison study was conducted between the PVP-capped palladium nanoparticles and the PAMAM-OH Generation 4 dendrimer-capped palladium nanoparticles.[18] The dendrimer strongly encapsulates the nanoparticles without fully passivating the nanoparticle surface. The PAMAM-OH Generation 4 dendrimer-capped nanoparticles were prepared using the sodium borohydride reduction method that takes place at room temperature for an hour,[18] while the PVP-capped nanoparticles studied previously[6] were prepared using the ethanol reduction

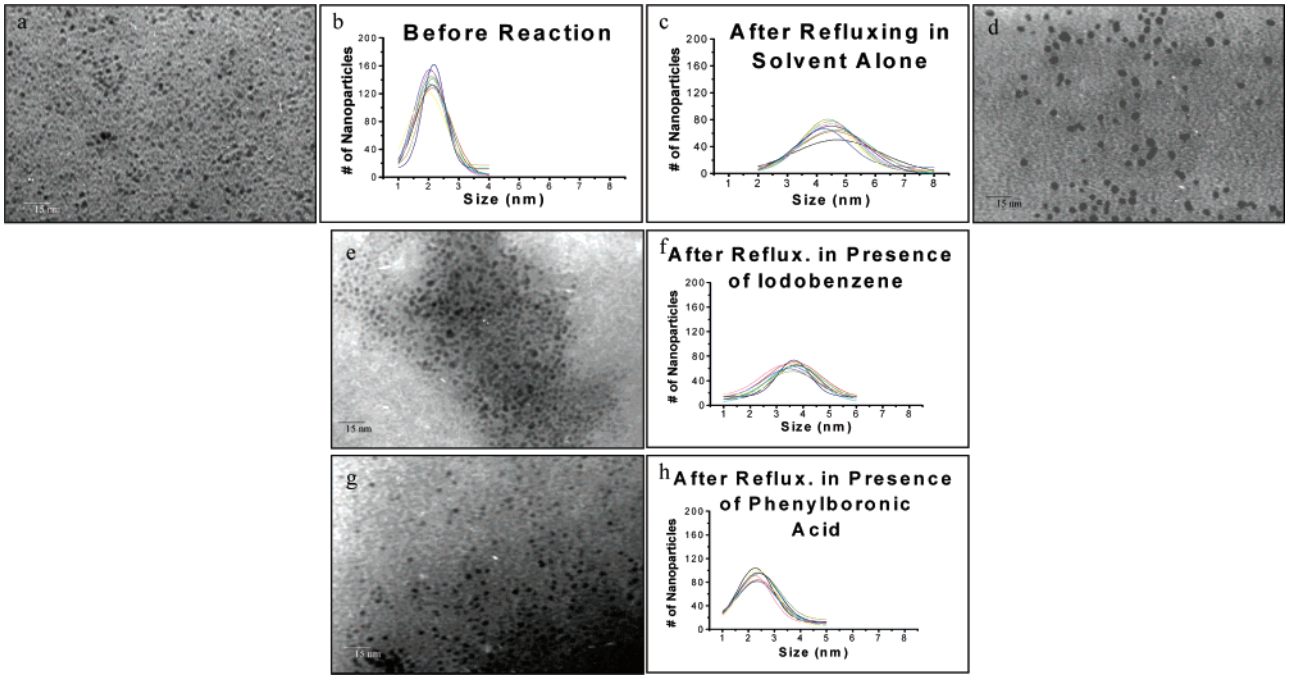

Figure 9. Effect of individual reactants on the size of the PVP-capped palladium nanoparticles. TEM images and Gaussian fits of the size distributions of the PVP−Pd nanoparticles before any perturbations (a−b), after refluxing the nanoparticles in just the 3:1 acetonitrile/water solvent (c−d), after refluxing the nanoparticles in the presence of iodobenzene (e−f), and after refluxing the nanoparticles in the presence of phenylboronic acid (g−h).[6] It is observed that the Ostwald ripening process takes place in the presence of the solvent alone and also in the presence of iodobenzene, one of the reactants. The Ostwald ripening process is greatly inhibited in the presence of phenylboronic acid, the other reactant.

method that takes place at reflux temperature for 3 h. The goal of the comparison study was to find out if the stabilizer used to cap the nanoparticles or the nanoparticle preparation method has any effect on the size of the palladium nanoparticles after catalyzing the Suzuki cross-coupling reaction.

When the dendrimer-capped palladium nanoparticles were used as catalysts for this reaction,[18] it was observed that the nanoparticles grew larger after both the first and second cycle, as can be seen in Figure 10. In the case of the PVP−Pd nanoparticles, aggregation and precipitation of the nanoparticles occurred during the second cycle. It is important to note that different methods of preparing nanoparticles will result in varying degrees of conversion of metal ions into capped nanoparticles. As a result, the two methods of synthesizing the nanoparticles will result in varying amounts of unreduced and partly reduced Pd ions left in solution after the synthetic process. Since the dendrimer-capped Pd nanoparticles are prepared using a milder reduction method, the conversion to full nanoparticles could be slower, resulting in a more incomplete reduction, which would result in more ions present in solution that could contribute to the growth process during the second cycle of the Suzuki reaction. In addition, the Generation 4 PAMAM-OH dendrimer is a better stabilizer with a greater encapsulating action than the PVP polymer.[4] As a result, the dendrimer-capped Pd nanoparticles are also more resistant to aggregation and precipitation than the PVP−Pd nanoparticles. In the case of the dendrimer−Pd nanoparticles, the growth process is not dominantly due to Ostwald ripening and is mainly due to the presence of excess Pd ions and Pd atoms in solution.[18]

In the case of the dendrimer−Pd nanoparticles, it is also observed that the nanoparticle growth process is inhibited in the presence of phenylboronic acid and occurs in the presence of the iodobenzene.[18] This suggests that the mechanism of the Suzuki reaction involves the phenylboronic acid binding to the nanoparticle surface and reacting with iodobenzene via collisional processes. This is in agreement with the mechanism we proposed previously based on the studies with the spherical PVP−Pd nanoparticles[6] and the studies with the tetrahedral PVP−Pt nanoparticles.[13] This suggests that the mechanism of the Suzuki reaction is insensitive to the stabilizer used to cap the nanoparticles.

The recycling potential of the dendrimer−Pd nanoparticles[18] was also investigated and compared to that of the PVP−Pd nanoparticles.[6] It was observed that the catalytic activity of the dendrimer-capped palladium nanoparticles is lower during the second cycle,[18] but not as much as observed with the PVP−Pd nanoparticles, based on a comparison of biphenyl ratios as shown in Table 3. A possible reason the biphenyl ratios are higher for the dendrimer−Pd nanoparticles is that the nanoparticles continue to grow during the second cycle, resulting in more active sites, since these sites are less likely to be poisoned by biphenyl. In addition, due to continued growth, precipitation of the nanoparticles is not taking place, which is also supported by the fact that Pd black was not observed after the second cycle of the reaction.

7. Conclusions

In the case of using colloidal metal nanoparticles as catalysts, it has been shown that during the early stages of the electron transfer reaction where no shape changes occur, the catalytic activity is dependent on the shape of the nanocatalyst used. This is verified by correlation of the catalytic activity with the fraction of surface atoms located on the corners and edges of the three types of nanoparticles. However, during the full course of the electron transfer reaction, it has also been shown that there are shape changes in which there is dissolution of atoms from the corners and edges, which gives rise to corresponding changes in the activation energy. When the colloidal tetrahedral platinum nanoparticles are used to catalyze a relatively harsh reaction such as the Suzuki cross-coupling reaction, it is observed that more drastic shape changes occur such as the complete

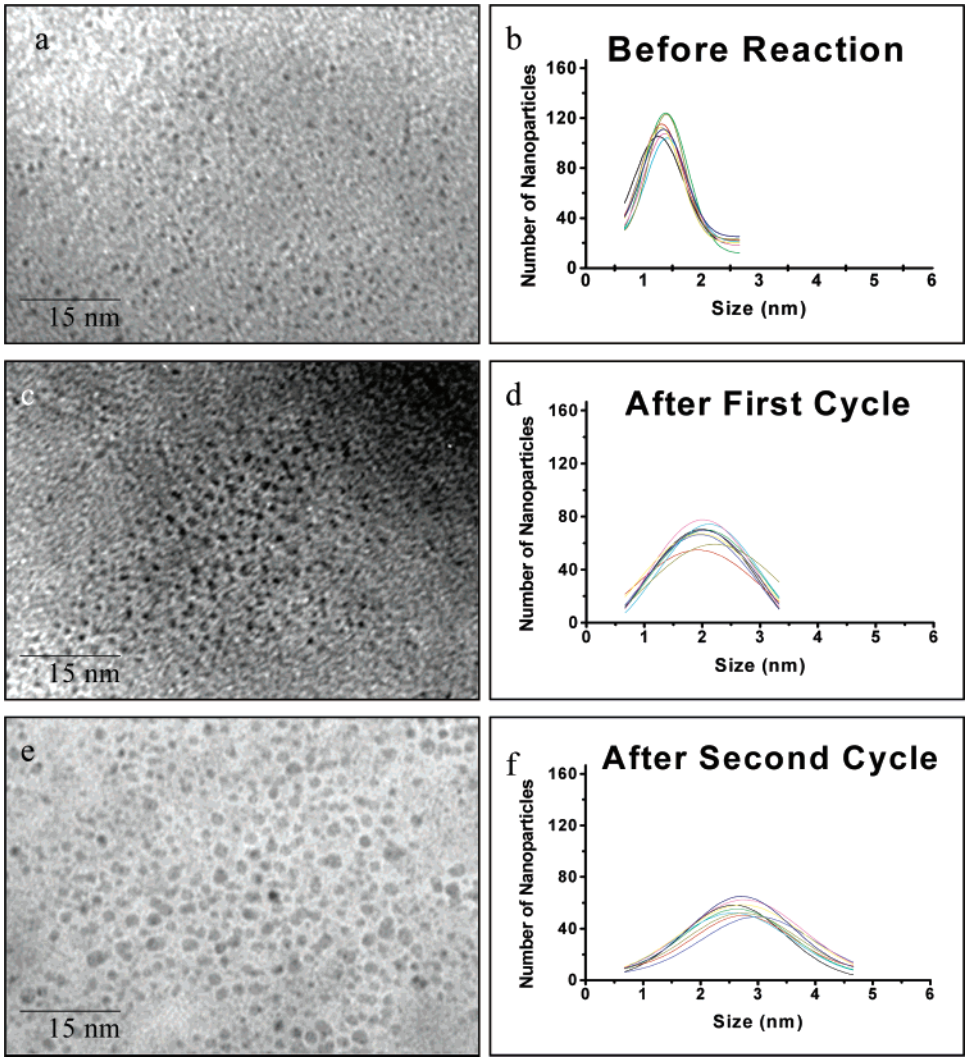

Figure 10. Effect of catalyzing the Suzuki reaction on the size of spherical dendrimer−Pd nanoparticles. TEM images and Gaussian fits of the size distributions of the spherical PAMAM−OH Generation 4 dendrimer-capped palladium nanoparticles before the reaction (a−b), after the first cycle of the Suzuki reaction (c−d), and after the second cycle of the Suzuki reaction (e−f).[18] When the dendrimer−Pd nanoparticles are used to catalyze the Suzuki reaction, it is observed that the nanoparticles grow larger in size during both the first and second cycle of the Suzuki reaction.

TABLE 3: Comparison of the Biphenyl Yield Ratios Obtained When the PVP−Pd Nanoparticles[6] and PAMAM-OH Generation 4 Dendrimer−Pd Nanoparticles[18] Are Used as Catalysts for the Suzuki Reaction

nanoparticle type	biphenyl yield ratio (2nd cycle/1st cycle)
spherical PVP−Pd nanoparticles	0.38 ± 0.08
spherical PAMAM-OH Generation 4 dendrimer−Pd nanoparticles	0.50 ± 0.09

transformation in the nanoparticle shape from tetrahedral to spherical. This drastic shape change also results in a dramatic reduction in the catalytic activity during the second cycle.

The use of spherical palladium nanoparticles to catalyze the Suzuki reaction resulted in the nanoparticles growing in size during the course of the reaction. The nanoparticle preparation method and stabilizer play a role in the amount of growth that occurs during the course of the Suzuki reaction. In addition, the spherical palladium nanoparticles are not very efficient catalysts in terms of its recycling potential. Investigations on the effect of individual reactants on the nanoparticle size and shape have provided important clues on the mechanism of both the electron-transfer reaction and the Suzuki cross-coupling reaction.

Acknowledgment. We acknowledge the NSF chemistry division (#0240380) for funding. We thank the Georgia Tech Electron Microscopy Center for the TEM and HRTEM microscopes we used to carry out this work. We also thank Dr. Gary Schuster's group for the reversed-phase HPLC we used to carry out the catalytic studies for the Suzuki reaction.

References and Notes

(1) Teranishi, T.; Miyake, M. *Chem. Mater.* **1998**, *10*, 594.
(2) Li, Y.; Hong, X. M.; Collard, D. M.; El-Sayed, M. A. *Org. Lett.* **2000**, *2*(15), 2385.
(3) Li, Y.; Boone, E.; El-Sayed, M. A. *Langmuir* **2002**, *18*, 4921.
(4) Li, Y.; El-Sayed, M. A. *J. Phys. Chem. B* **2001**, *105*, 8938.
(5) Shiraishi, Y.; Nakayama, M.; Takagi, E.; Tominaga, T.; Toshima, M. *Inorg. Chim. Acta* **2000**, *300*−*302*, 964.
(6) Narayanan, R.; El-Sayed, M. A. *J. Am. Chem. Soc.* **2003**, *125*(27), 8340.
(7) Narayanan, R.; El-Sayed, M. A. *J. Phys. Chem. B* **2003**, *107*(45), 12416.
(8) Ahmadi, T. S.; Wang, Z. L.; Green, T. C.; Henglein, A.; El-Sayed, M. A. *Science* **1996**, *272*, 1924.
(9) Yu, Y.; Xu, B. *Chin. Sci. Bull.* **2003**, *48*(23), 2589.
(10) Narayanan, R.; El-Sayed, M. A. *J. Phys. Chem. B* **2004**, *108*(18), 5726.
(11) Narayanan, R.; El-Sayed, M. A. *Nano Lett.* **2004**, *4*(7), 1343.
(12) Narayanan, R.; El-Sayed, M. A. *J. Am. Chem. Soc.* **2004**, *126*(23), 7194.
(13) Narayanan, R.; El-Sayed, M. A. *Langmuir* **2005**, *21*(5), 2027.

(14) Sau, T. K.; Pal, A.; Pal, T. *J. Phys. Chem. B* **2001**, *105*(38), 9266.
(15) Crooks, R. M.; Zhao, M.; Sun, L.; Chechik, V.; Yeung, L. K. *Acc. Chem. Res.* **2001**, *34*, 181.
(16) Schulz, J.; Roucoux, A.; Patin, H. *Chem. Eur. J.* **2000**, *6*(4), 618.
(17) Mayer, A. B. R.; Hausner, S. H.; Mark, J. E. *Polym. J.* **2000**, *32*, 15.
(18) Narayanan, R.; El-Sayed, M. A. *J. Phys. Chem B* **2004**, *108*(25), 8572.
(19) Reetz, M. T.; Helbig, W. *J. Am. Chem. Soc.* **1994**, *116*, 7401.
(20) Reetz, M. T.; Quaiser, S. A. *Angew. Chem., Int. Ed. Engl.* **1995**, *34*, 2240.
(21) Michaelis, M.; Henglein, A. *J. Phys. Chem.* **1992**, *96*, 4719.
(22) Toshima, N.; Takahashi, T.; Hirai, H. *Chem. Lett.* **1985**, 1245.
(23) Kurihara, K.; Kizling, J.; Stenius, P.; Fendler, J. H. *J. Am. Chem. Soc.* **1983**, *105*, 2574.
(24) Nagata, Y.; Watanabe, Y.; Fujita, S.; Dohmaru, T.; Taniguchi, S. *J. Chem. Soc., Chem. Commun.* **1992**, 1620.
(25) Caruso, R. A.; Ashokkumar, M.; Grieser, F. *Colloids Surf. A* **2000**, *169*, 219.
(26) Fujimoto, T.; Terauchi, S.; Umehara, H.; Kojima, I.; Henderson, W. *Chem. Mater.* **2001**, *13*, 1057.
(27) Borsla, A.; Wilhelm, A. M.; Delmas, H. *Catal. Today* **2001**, *66*(2−4), 389.
(28) Sulman, E.; Lakina, N.; Sulman, M.; Ankudinova, T.; Matveeva, V.; Sidorov, A.; Sidorov, S. *Stud. Surf. Sci. Catal.* **2000**, *130B*, 1787.
(29) Scott, R. W. J.; Datye, A. K.; Crooks, R. M. *J. Am. Chem. Soc.* **2003**, *125*(13), 3708.
(30) Pittelkow, M.; Moth-Poulsen, K.; Boas, U.; Christensen, J. B. *Langmuir* **2003**, *19*(18), 7682.
(31) Bronstein, L. M.; Chernyshov, D. M.; Volkov, I. O.; Ezernitskaya, M. G.; Valetsky, P. M.; Matveeva, V. G.; Sulman, E. M. *J. Calal.* **2000**, *196*(2), 302.
(32) Lu, Z.; Liu, G.; Phillips, H.; Hill, J. M.; Chang, J.; Kydd, R. A. *Nano Lett.* **2001**, *1*(12), 683.
(33) Bronstein, L. M.; Chernyshov, D. M.; Volkov, I. O.; Ezernitskaya, M. G.; Valetsky, P. M.; Matveeva, V. G.; Sulman, E. M. *J. Calal.* **2000**, *196*(2), 302.
(34) Aiken, J. D., III.; Finke, R. G. *J. Mol. Catal. A: Chem.* **1999**, *145*, 1.
(35) Mevellec, V.; Roucoux, A.; Ramirez, E.; Philippot, K.; Chaudret, B. *Adv. Synth. Catal.* **2004**, *346*(1), 72.
(36) Lin, Y.; Finke, R. G. *J. Am. Chem. Soc.* **1994**, *116*, 8335.
(37) Chen, S.; Kucernak, A. *J. Phys. Chem. B* **2004**, *108*(10), 3262.
(38) Liu, Z.; Ling, X. Y.; Lee, J. Y.; Su, X.; Gan, L. M. *J. Mater. Chem.* **2003**, *13*(12), 3049.
(39) Fachini, E. R.; Diaz-Ayala, R.; Casado-Rivera, E.; File, S.; Cabrera, C. R. *Langmuir* **2003**, *19*(21), 8986.
(40) Lang, H.; May, R. A.; Iversen, B. L.; Chandler, B. D. *J. Am. Chem. Soc.* **2003**, *125*(48), 14832.
(41) Bianchini, C.; Dal Santo, V.; Meli, A.; Moneti, S.; Moreno, M.; Oberhauser, W.; Psaro, R.; Sordelli, L.; Vizza, F. *J. Catal.* **2003**, *213*(1), 47.
(42) Yoo, J. W.; Hathcock, D. J.; El-Sayed, M. A. *J. Catal.* **2003**, *214*(1), 1.
(43) Yoo, J. W.; Hathcock, D.; El-Sayed, M. A. *J. Phys. Chem. A* **2002**, *106*(10), 2049.
(44) Marconi, G.; Pertici, P.; Evangelisti, C.; Caporusso, A. M.; Vitulli, G.; Capannelli, G.; Hoang, M.; Turney, T. W. *J. Organomet. Chem.* **2004**, *689*(3), 639.
(45) Bowker, M.; Stone, P.; Bennett, R.; Perkins, N. *Surf. Sci.* **2002**, *511*(1−3), 435.
(46) Claus, P.; Hofmeister, H. *J. Phys. Chem. B* **1999**, *103*(14), 2766.
(47) Chen, C.-W.; Serizawa, T.; Akashi, M. *Chem. Mater.* **1999**, *11*, 1381.
(48) Hirai, H.; Ohtaki, M.; Komiyama, M. *Chem. Lett.* **1986**, 269.
(49) Jacobs, P. W.; Wind, S. J.; Ribeiro, F. H.; Somorjai, G. A. *Surf. Sci.* **1997**, *372*(1−3), L249.
(50) Eppler, A.; Rupprechter, G.; Guczi, L.; Somorjai, G. A. *J. Phys. Chem. B* **1997**, *101*(48), 9973.
(51) Eppler, A. S.; Rupprechter, G.; Anderson, E. A.; Somorjai, G. A. *J. Phys. Chem. B* **2000**, *104*(31), 7286.
(52) Grunes, J.; Zhu, J.; Anderson, E. A.; Somorjai, G. A. *J. Phys. Chem. B* **2002**, *106*(44), 11463.
(53) Spiro, M.; De Jesus, D. *Langmuir* **2000**, *16*(6), 2464.
(54) Shiraishi, Y.; Toshima, N. *J. Mol. Catal. A: Chem.* **1999**, *141*, 187.
(55) Launay, F.; Roucoux, A.; Patin, H. *Tetrahedron Lett.* **1998**, *39*, 1353.
(56) Kogan, V.; Aizenshtat, Z.; Popovitz-Biro, R.; Neumann, R. *Org. Lett.* **2002**, *4*(20), 3529.
(57) Gopidas, K. R.; Whitesell, J. K.; Fox, M. A. *Nano Lett.* **2003**, *3*(12), 1757.
(58) Na, Y.; Park, S.; Han, S. B.; Han, H.; Ko, S.; Chang, S. *J. Am. Chem. Soc.* **2004**, *126*(1), 250.
(59) Yeung, L. K.; Crooks, R. M. *Nano Lett.* **2001**, *1*(1), 14.
(60) Calo, V.; Nacci, A.; Monopoli, A.; Laera, S.; Cioffi, N. *J. Org. Chem.* **2003**, *68*(7), 2929.
(61) Li, Y.; Petroski, J.; El-Sayed, M. A. *J. Phys. Chem. B* **2000**, *104*(47), 10956.
(62) Sharma, R. K.; Sharma, P.; Maitra, A. *J. Coll. Interface Sci.* **2003**, *265*(1), 134.
(63) Freund, P. L.; Spiro, M. *J. Phys. Chem.* **1985**, *89*, 1074.
(64) Ohde, H.; Ohde, M.; Wai, C. M. *Chem. Commun.* **2004**, *8*, 930.
(65) Anderson, K.; Cortinas Fernandez, S.; Hardacre, C.; Marr, P. C. *Inorg. Chem. Commun.* **2003**, *7*(1), 73.
(66) Adlim, M.; Abu Bakar, M.; Liew, K. Y.; Ismail, J. *J. Mol. Catal. A: Chem.* **2004**, *212*(1−2), 141.
(67) Somorjai, G. A. *Appl. Surf. Sci.* **1997**, *121/122*, 1.
(68) Boudjahem, A. G.; Monteverdi, S.; Mercy, M.; Bettahar, M. M. *J. Catal.* **2004**, *221*(2), 325.
(69) Claus, P.; Hofmeister, H. *J. Phys. Chem. B*, **1999**, *103*(14), 2766.
(70) Anderson, M. L.; Stroud, R. M.; Rolison, D. R. *Nano Lett.* **2002**, *2*(3), 235.
(71) Long, J. W.; Stroud, R. M.; Swider-Lyons, K. E.; Rolison, D. R. *J. Phys. Chem. B* **2000**, *104*, 9772.
(72) Moore, J. T.; Corn, J. D.; Chu, D.; Jiang, R.; Boxall, D. L.; Kenik, E. A.; Lukehart, C. M. *Chem. Mater.* **2003**, *15*(17), 3320.
(73) Bradley, J. S. *Cluster Colloids* **1994**, 459.
(74) Duff, D. G.; Baiker, A. *Stud. Surf. Sci. Catal.* **1995**, *91*, 505.
(75) Toshima, N. *NATO ASI Ser., Ser. 3* **1996**, *12*, 371.
(76) Boennermann, H.; Braun, G.; Brijoux, G. B.; Brinkman, R.; Tilling, A. S.; Schulze, S. K.; Siepen, K. *J. Organomet. Chem.* **1996**, *520*(1−2), 143.
(77) Fugami, K. *Organomet. News* **2000**, *1*, 25.
(78) Mayer, A. B. R. *Polym. Adv. Technol.* **2001**, *12*(1−2), 96.
(79) Bonnemann, H.; Richards, R. *Synth. Methods Organomet. Inorg. Chem.* **2002**, *10*, 209.
(80) Moiseev, I. I.; Vargaftik, M. N. *Russ. J. Chem.* **2002**, *72*(4), 512.
(81) Eppler, A.; Rupprechter, G.; Guczi, L.; Somorjai, G. A. *J. Phys. Chem. B* **1997**, *101*(48), 9973.
(82) Toshima, N.; Yonezawa, T. *New J. Chem.* **1998**, *22* (11), 1179.
(83) Schmid, G. *Met. Cluster Chem.* **1999**, *3*, 1325.
(84) Puddephatt, R. J. *Met. Cluster Chem.* **1999**, *2*, 605.
(85) Henry, C. R. *Appl. Surf. Sci.* **2000**, *164*, 252.
(86) St. Clair, T. P.; Goodman, D. W. *Top. Catal.* **2000**, *13*(1,2), 5.
(87) Kralik, M.; Corain, B.; Zecca, M. *Chem. Pap.* **2000**, *54*(4), 254.
(88) Chusuei, C. C.; Lai, X.; Luo, K.; Goodman, D. W. *Top. Catal.* **2001**, *14*(1−4), 71.
(89) Bowker, M.; Bennett, R. A.; Dickinson, A.; James, D.; Smith, R. D.; Stone, P. *Stud. Surf. Sci. Catal.* **2001**, *133*, 3.
(90) Kralik, M.; Biffis, A. *J. Mol. Catal. A: Chem.* **2001**, *177*(1), 113.
(91) Thomas, J. M.; Raja, R. *Chem. Rec.* **2001**, *1*(6), 448.
(92) Mohr, C.; Claus, P. *Sci. Prog.* **2001**, *84*(4), 311.
(93) Thomas, J. M.; Johnson, B. F. G.; Raja, R.; Sankar, G.; Midgley, P. A. *Acc. Chem. Res.* **2003**, *36*(1), 20.
(94) Sculz, J.; Roucoux, A.; Patin, H. *Chem. Eur. J.* **2000**, *6*(4), 618.
(95) Collier, P. J.; Iggo, J. A.; Whyman, R. *J. Mol. Catal. A: Chem.* **1999**, *146*(1−2), 149.
(96) Wang, Q.; Liu, H.; Han, M.; Li, X.; Jiang, D. *J. Mol. Catal. A: Chem.* **1997** *118*(2), 145.
(97) Sidorov, S. N.; Volkov, I. V.; Davankov, V. A.; Tsyurupa, M. P.; Valetsky, P. M.; Bronstein, L. M.; Karlinsey, R.; Zwanziger, J. W.; Matveeva, V. G.; Sulman, E. M.; Lakina, N. V.; Wilder, E. A.; Spontak, R. J. *J. Am. Chem. Soc.* **2001** *123*(43), 10502.
(98) Roucox, A:, Sculz, J.; Patin, H. *Chem. Rev.* **2002**, *102*(10), 3757.
(99) Chechik, V.; Crooks, R. M. *J. Am. Chem. Soc.* **2000**, *122*, 1243.
(100) Yeung, L. K.; Crooks, R. M. *Nano Lett.* **2001**, *1*(1), 14.
(101) Dupont, J.; Fonseca, G. S.; Umpierre, A. P.; Fichtner, P. F. P.; Teixeira, S. R. *J. Am. Chem. Soc.* **2002**, *124*, 4228.
(102) Hirai, H.; Chawanya, H.; Toshima, N. *Nippon Kagaku Kaishi* **1984**, *6*, 1027.
(103) Fu, X.; Wang, Y.; Wu, N.; Gui, L.; Yang, Y. *Langmuir* **2002**, *18*(12), 4619.
(104) Chen, J.; Herricks, T.; Geissler, M.; Xia, Y. *J. Am. Chem. Soc.* **2004**, *126*, 10854.
(105) Herricks, T.; Chen, J.; Xia, Y. *Nano Lett.* **2004**, *4*(12), 2367.
(106) Freund, P. L.; Spiro, M. *J. Phys. Chem.* **1985**, *89*, 1074.
(107) Freund, P. L.; Spiro, M. *J. Chem. Soc., Faraday Trans.* **1986**, *82*, 2277.
(108) Clint, J. H.; Collins, I. R.; Williams, J. A.; Robinson, B. H.; Towey, T. F.; Cajean, P.; Khan-Lodhi, A. *Faraday Discuss.* **1993**, *95*, 219.
(109) Hardeveld, R. V.; Hartog, F. *Surf. Sci.* **1969**, *15*, 189.
(110) Miyaura, N.; Yanagi, T.; Suzuki, A. *Synth. Commun.* **1981**, *11*, 513.

(111) Suzuki, A. In *Metal-Catalyzed Cross-Coupling Reactions*; Diederich, F., Stang, P. J., Eds.; VCH: Weinheim, 1998; p 49.
(112) Alo, B. I.; Kandil, A.; Patil, P. A.; Sharp, M. J.; Siddiqui, M. A.; Snieckus, V. *J. Org. Chem.* **1991**, *56*, 3763.
(113) Wallow, T. I.; Novak, B. M. *J. Org. Chem.* **1994**, *59*, 5034.
(114) Bumagin, N. A.; Bykov, V. V.; Beletskaya, I. P.; *Dokl. Akad. Nauk. SSSR* **1990**, *315*, 1133.
(115) Marck, G.; Villiger, A.; Buchecker, R. *Tetrahedron Lett.* **1994**, *35*, 3277.
(116) Reetz, M. T.; Breinbauer, R.; Wanninger, K. *Tetrahedron Lett.* **1996**, *26*, 4499.
(117) Moreno-Manas, M.; Pleixats, R.; Villarroya, S. *Organomet.* **2001**, *20*(22), 4524.
(118) Kogan, V.; Aizenshtat, Z.; Popovitz-Biro, R.; Neumann, R. *Org. Lett.* **2002**, *4*(20), 3529.
(119) Strimbu, L.; Liu, J.; Kaifer, A. E. *Langmuir* **2003**, *19*, 483.
(120) Colacot, T. J.; Qian, H.; Cea-Olivares, R.; Hernandez-Ortega, S. *J. Organomet. Chem.* **2001** *637*−*639*, 691.
(121) Thathagar, M. B.; Beckers, J.; Rothenberg, G. *J. Am. Chem. Soc.* **2002**, *124*(40), 11858.
(122) Howard, A.; Mitchell, C. E. J.; Egdell, R. G. *Surf. Sci.* **2002**, *515*, L504.
(123) Imre, A.; Beke, D. L.; Gontier-Moya, E.; Szabo, I. A.; Gillet, E. *Appl. Phys. A* **2000**, *71*, 19.
(124) Diana, F. S.; Lee, S.-H.; Petroff, P. M.; Kramer, E. J. *Nano Lett.* **2003**, *3*(7), 891.
(125) Peng, X.; Wickham, J.; Alivisatos, A. P. *J. Am. Chem. Soc.* **1998**, *120*, 5343.
(126) Liu, F.-K.; Huang, P.-W.; Chang, Y.-C.; Ko, C.-J.; Ko, F.-H.; Chu, T.-C. *J. Cryst. Growth* **2005**, *273*, 439.
(127) Sun, Y.; Gates, B.; Mayers, B.; Xia, Y. *Nano Lett.* **2002**, *2*(2), 165.
(128) Manna, L.; Scher, E. C.; Alivisatos, A. P. *J. Am. Chem. Soc.* **2000**, *122*, 12700.